Electrochemistry Communications 11 (2009) 695–698

Contents lists available at ScienceDirect

Electrochemistry Communications

journal homepage: www.elsevier.com/locate/elecom

XPS/EXAFS study of cycleability improved $LiMn_2O_4$ thin film cathodes prepared by solution deposition

Dong Wook Shin [a,b], Ji-Won Choi [a,*], Won-Kook Choi [c], Yong Soo Cho [b], Seok-Jin Yoon [a]

[a] Thin Film Materials Research Center, Korea Institute of Science and Technology, 39-1 Hawolgok, Seongbuk, Seoul 136-791, Republic of Korea
[b] Department of Materials Science and Engineering, Yonsei University, Seoul 120-749, Republic of Korea
[c] Materials Science and Technology Research Division, Korea Institute of Science and Technology, Seoul 136-791, Republic of Korea

ARTICLE INFO

Article history:
Received 9 December 2008
Received in revised form 12 January 2009
Accepted 13 January 2009
Available online 20 January 2009

Keywords:
Spinel
Cathode
Sn substitution
Solution deposition
Cycleability

ABSTRACT

The influence of Sn substitution in $LiMn_2O_4$ thin films as a cathode has been studied via solution deposition to improve the electrochemical performance of thin film lithium batteries. $LiSn_{0.025}Mn_{1.95}O_4$ thin films showed the most promising performance, i.e. a high capacity retention of 77% at 10 C after the 500th cycle, due to the increased average Mn valence state. The thin films of $LiSn_{x/2}Mn_{2-x}O_4$ ($x \geqslant 0.10$) showed significant precipitation of SnO_2 and SnO after the cycling evaluation.

1. Introduction

Thin film lithium-ion cells have been regarded as one of the next generation power sources for future ubiquitous environments. The high production cost and chemical instability of the cells have been the critical issues particularly for small-scale, portable, and semi-permanent applications [1–3]. As an alternative cathode material to commercially-available $LiCoO_2$, $LiMn_2O_4$ has been known to be less toxic, cheaper, and safer during the cell operation. $LiMn_2O_4$ still has some issues to be overcome for commercialization, which include a gradual loss in discharge capacity with increasing the number of the charge–discharge cycle. The loss is known to originate from structural instability, which is induced by the Mn dissolution into electrolyte and the known Jahn–Teller transition of the cubic to tetragonal [4]. The spinel lithium manganese oxide has a distorted spinel structure. The distortion can be increased by substituent, which was intended to enhance the cycleability of the cathode by increasing the average valence number of Mn [5]. Accordingly, desirable compositional modifications have been demanded for the purpose of enhancing the average valence state of Mn while minimizing the degree of distortion in the spinel structure. This work deals with Sn-substituted $LiMn_2O_4$ thin films, corresponding to $LiSn_{x/2}Mn_{2-x}O_4$ ($x = 0$, 0.05, 0.1, and 0.2), primarily for overcoming the serious degradation in the discharge capacity of $LiMn_2O_4$. The thin films prepared on a $Pt/Ti/SiO_2/Si(100)$ substrate by spin coating of chemical solutions were investigated in regards to structural and electrochemical characteristics with the support of several analytical techniques including XRD (X-ray diffraction), XPS (X-ray photoelectron spectroscopy), and EXAFS (extended X-ray absorption fine structure).

2. Experimental

Thin films were prepared on a $Pt/Ti/SiO_2/Si(100)$ substrate by solution deposition. Lithium acetylacetonate $CH_3COCHC(OLi)CH_3$, manganese (III) acetylacetonate $Mn(C_5H_7O_2)_3$, and tin (II) acetate $Sn(CH_3CO_2)_2$ were completely dissolved into a common solution of 1-butanol and acetic acid by stirring for 20 h. A solution of 0.3 M was used for spin coating on $Pt/Ti/SiO_2/Si(100)$ substrates. The steps of spin coating and preheating at 310 °C were repeated up to eight times. The films were finally annealed at 750 °C for 5 min in O_2 atmosphere using a rapid thermal processor (KVT, KVRTA-R40). The thickness of films was ~140 nm. Electrochemical measurements were carried out, using a lab-made half cell unit. Electrolyte was a 1 M solution of $LiPF_6$ based on a 1:1 vol% mixture of ethylene carbonate (EC) and diethyl carbonate (DEC). The counterelectrode was a lithium metal foil. The charge/discharge was performed at a current density of 300 mA/g between 3.0 and 4.5 V. XPS spectra were collected on a PHI 5800 ESCA System with a monochromatic Al $K\alpha$ (1486.6 eV) anode (250 W, 10 kV, 27 mA). The deconvolutions of narrow scan peaks of Mn 2*p* and Sn 3*d*

* Corresponding author. Tel.: +82 2 958 5556; fax: +82 2 958 6720.
E-mail address: jwchoi@kist.re.kr (J.-W. Choi).

1388-2481/$ - see front matter © 2009 Elsevier B.V. All rights reserved.
doi:10.1016/j.elecom.2009.01.019

core-levels related to each portion of Mn^{3+}, Mn^{4+}, Sn^{2+}, and Sn^{4+} are performed by the program of SDP 4.0 (XPS international, LLC) with a condition using Shirley baseline and 90/10% ratio of Gaussian/Lorentzian function. Mn *K* edge X-ray absorption spectra were recorded on a 3C1 beam line at Pohang Light Source (PLS) with a ring current of 130–185 mA at 2.5 GeV. A Si(1 1 1) double-crystal monochromator was employed. All spectra were recorded in transmission mode using N_2 filled ionization chamber and calibrated by checking the first inflection point of Mn foil, Mn *K* edge = 6539 eV, as a reference. Fourier transformations (FT) were performed using k^2 weighting. Theoretical parameters used in the curve-fitting analysis were calculated by the program of FEFF 7.0. An X-ray diffractometer (Rigaku, RINT 2000) using Cu $K\alpha$ radiation was used for phase identification.

3. Results and discussion

Fig. 1a shows the cycleability of $LiSn_{x/2}Mn_{2-x}O_4$ thin films ($x = 0$, 0.05, 0.1, and 0.2) up to 500 cycles. The capacity retention of the $x = 0.05$ thin film was 77% of the first discharge capacity after 500 cycles at the higher current density of 10 C. The high current density of 10 C which corresponds to the current rate of 300 mA/g has been found to differentiate cycleability among samples certainly.

Fig. 1b shows the X-ray diffraction patterns of $LiSn_{x/2}Mn_{2-x}O_4$ thin films prepared by the solution deposition process before and after the third cycle. It was shown that all films had the identical cubic phase with space group $Fd\bar{3}m$ regardless of Sn content. No distinguishable secondary phase was observed at $x = 0.05$. When Sn content was $x \geqslant 0.1$, however, precipitation peaks of both SnO_2 (1 1 0) and SnO (1 1 0) were observed. The precipitation peaks of SnO_2 (1 1 0) and SnO (1 1 0) were observed apparently for the samples of $x \geqslant 0.1$ after the cycling test. It is thought that SnO_2 and SnO precipitated as an accompanying result of the Mn dissolution as well as SnO_2 and SnO located out of the $LiMn_2O_4$ lattice, which originated from the disproportionation reaction during the cycling test [6]. The disproportionation reaction was reported in other similar systems including yttrium-doped spinel $LiMn_2O_4$, where the substituting ions facilitated the dissolution of Mn [7].

Fig. 2a shows the XPS spectra of Mn $2p_{1/2}$ and Mn $2p_{3/2}$ core-levels of $LiSn_{x/2}Mn_{2-x}O_4$ thin films which result from the spin-orbit splitting. Larger FWHM (full width at half maximum) than 3.5 eV of all the Mn $2p_{3/2}$ peaks explicitly indicates coexistence of mixed Mn^{3+} and Mn^{4+} ions over the substitution range of Sn. Deconvoluted Mn XPS profiles in Fig. 2b denote the each percentage of manganese content, which can be used to calculate the average valance states of Mn between Mn^{3+} and Mn^{4+}. Deconvolution was precisely carried out at the conditions of the binding energy positions of Mn^{3+} and Mn^{4+} fixed at 642.1 and 643.6 eV, respectively and the FWHM lower than 4.0 eV. The $x = 0.05$ sample can be highlighted with a valence state of 3.61, which is higher than the 3.50 value of pure thin films and the valance state becomes small as much as 3.56 and 3.50 at higher Sn contents of $x = 0.1$ and 0.2, respectively. It is assumed that such a slight increase in valence state at $x = 0.05$ sample is associated with the replacement of Mn^{3+} in the octahedral site (16*d*) with Sn^{2+} (Sn'_{Mn}) and Mn vacancy (V'''_{Mn}) to maintain charge neutrality.

Fig. 2c shows the XPS spectra of Sn $3d_{3/2}$ and Sn $3d_{5/2}$ core-levels of $LiSn_{x/2}Mn_{2-x}O_4$ thin films which result from the spin-orbit splitting. The peak points of both Sn$3d_{3/2}$ and Sn$3d_{5/2}$ core-levels are shifted to lower binding energies as Sn content increases. This tendency means that the relative content of Sn^{2+} is more than that of Sn^{4+} at higher Sn contents. The each percentage of Sn content could be identified more definitely from deconvolution profiles in Fig. 2d. The deconvolution was precisely carried out at the conditions of fixing the binding energy positions of Sn^{2+} and Sn^{4+} at 485.75 and 486.75 eV with the FWHM lower than 1.4 eV, respectively [8].

If all components of Sn^{2+} and Sn^{4+} substitute Mn, the average valence state of Mn by the calculation from Sn deconvolution data in Fig. 2d is 3.62, 3.71, and 3.91 at $x = 0.05$, 0.1, and 0.2.

This behavior of the average charge state of Mn can be understood from comparing the ionic radii of Sn and Mn because the relation of the ionic radii is Sn^{2+} (0.930 Å)>Mn^{3+} (0.785 Å)>Sn^{4+} (0.690 Å)>Mn^{4+} (0.670 Å) [9]. Considering the charge affinities and sizes of Sn and Mn ions, Sn^{2+} and Sn^{4+} can effectively substitute Mn^{3+} and Mn^{4+}, respectively. The average valence of Mn increases when Sn^{2+} substitutes Mn^{3+}, whereas that of Mn decreases when Sn^{4+} substitutes Mn^{4+}. As shown in Fig. 1b, the intensity of SnO (1 1 0) peak increases at a higher rate than SnO_2 (1 1 0) peak as the increase in Sn content. It means that a small amount of Sn^{2+} substitutes Mn^{3+} at a limited solubility and most of the Sn^{2+} locates out of $LiMn_2O_4$ lattice due to the large ionic radius of Sn^{2+}. On the other hand, more Sn^{4+} is assumed to substitute Mn^{4+} rather than Sn^{2+} does Mn^{3+}. Therefore, the average valence state of Mn decreases at $x \geqslant 0.1$.

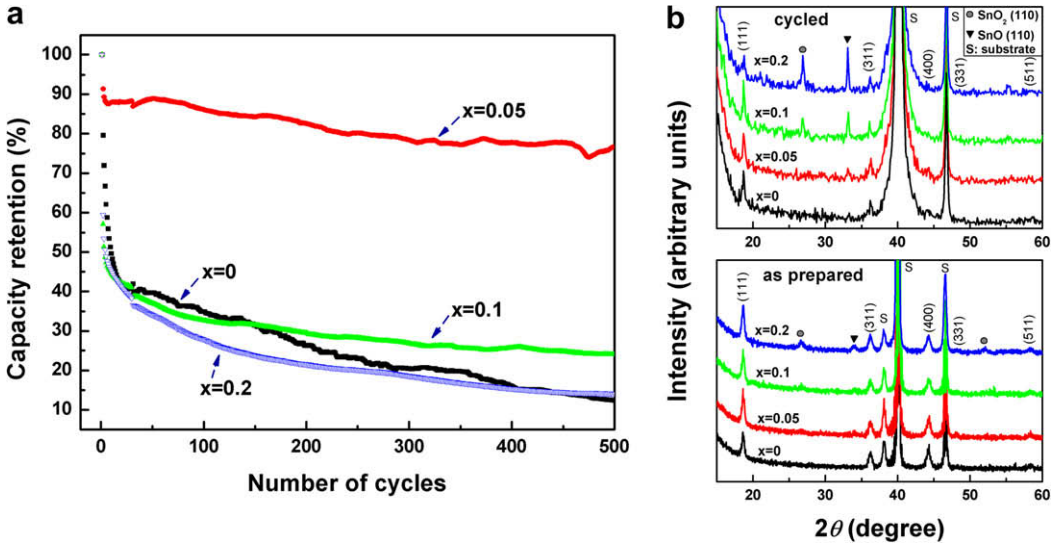

Fig. 1. (a) Capacity retention of $LiSn_{x/2}Mn_{2-x}O_4$ thin films up to 500 cycles and (b) XRD patterns of $LiSn_{x/2}Mn_{2-x}O_4$ thin films as prepared and after the third cycle.